

EasiCSDeep: A deep learning model for Cervical Spondylosis Identification using surface electromyography signal

Nana Wang^{1,2}, Li Cui^{1,4}, Xi Huang¹, Yingcong Xiang^{1,2}, Jing Xiao³

¹*Institute of Computing Technology(ICT), Chinese Academy of Sciences(CAS), Beijing, China.*

²*University of Chinese Academy of Sciences, Beijing, China.*

³*Xiyuan Hospital, China Academy of Chinese Medical Sciences(CACMS), Beijing, China.*

⁴*e-mail:lcui@ict.ac.cn.*

Cervical spondylosis (CS) is a common chronic disease that affects up to two-thirds of the population and poses a serious burden on individuals and society. The early identification has significant value in improving cure rate and reducing costs. However, the pathology is complex, and the mild symptoms increase the difficulty of the diagnosis, especially in the early stage. Besides, the time-consuming and costliness of hospital medical service reduces the attention to the CS identification. Thus, a convenient, low-cost intelligent CS identification method is imperious demanded. In this paper, we present an intelligent method based on the deep learning to identify CS, using the surface electromyography (sEMG) signal. Faced with the complex, high dimensionality and weak usability of the sEMG signal, we proposed and developed a multi-channel EasiCSDeep algorithm based on the convolutional neural network, which consists of the feature extraction, spatial relationship representation and classification algorithm. To the best of our knowledge, this EasiCSDeep is the first effort

to employ the deep learning and the sEMG data to identify CS. Compared with previous state-of-the-art algorithm, our algorithm achieves a significant improvement.

1 Introduction

The cervical spondylosis(CS) is a common degenerative disease that harm human life and health, affects up to two-thirds of the population, and pose an serious burden on individuals and society¹⁻⁴.

The early identification is an effective means to improve the cure rate and reduce the cost. However, the CS identification is difficult by analyzing the clinical symptom and the spinal lesions for the following reasons: (1) the CS is a complex disease associated with a series of clinical symptom¹ and the spinal lesions². (2) there are many cases of cervical lesions in asymptomatic patients⁷.

What's more, as the clinical symptoms and the spinal lesions of the early stages are relatively mild, the difficulty of the diagnosis increase. In addition, as the mild clinical symptoms of the early stages usually do not affect the live and work, it is easily overlooked by the suffers. Meanwhile, the chronic degenerative disease CS will worsen over time if not intervened as early as possible. Thus, the early identification is an essential, significant and an challenging task that need be paid more attention.

Currently, the clinical diagnosis mainly depend on the doctor's judgment from the clinical

¹The clinical symptoms include neck and back pain, upper limb weakness, head halo nausea, vomiting, numbness of fingers, weakness of lower limbs, difficulty in walking, even tachycardia, difficulty in swallowing, blurred vision, etc^{5,6}.

²The spinal lesions include the vertebral bodies and intervertebral disks degeneration, disk ruptures, herniation, etc⁴. Usually, as cervical degeneration worsens, clinical manifestations become more obvious.

symptoms and spinal lesions provided by expensive instruments in hospital ⁴, which rely on the intervention of medical resources including the professionals and medical instruments. However, the time-consuming and high cost of hospital medical service reduce people's attention to the early CS identification even if the suffers feel slightly uncomfortable in neck. Meanwhile, the early identification is also hindered by the problem of difficulty and expensive to access medical service caused by the insufficient and uneven distribution of health care resources considering the population ⁸⁻¹³. In detail, a large number of patients from all over the country flocked to the hospital with high-quality medical resources for medical service, exceeding the normal reception capacity of the hospital. The transportation, enrollment and queuing brings great inconvenience to the diagnosis and treatment of diseases, even delaying the diagnosis and treatment. Besides, the expenditure is caused by the transportation and accommodation, further increasing the burden. With the development of the artificial intelligence(AI), it provides an opportunity for the people to seek a convenient, low-cost medical server. The artificial intelligence algorithm are used to realize the movable or even family of cervical spondylosis identification services, providing the convenient, low-cost service. As the current common means, the image-based intelligent CS identification attracts a lot of attention ^{4,14,15}. Though it is the most intuitive, accurate and human resource-saving method at present, the dependence on medical instruments resources makes this method inconvenience and costly. A CS identification method is urgently needed, which enables people to conveniently and timely receive medical services at low cost to prompt the early identification and treatment of the CS.

Fortunately, with the development of the biomedical electrode manufacturing technology ¹⁶⁻²¹,

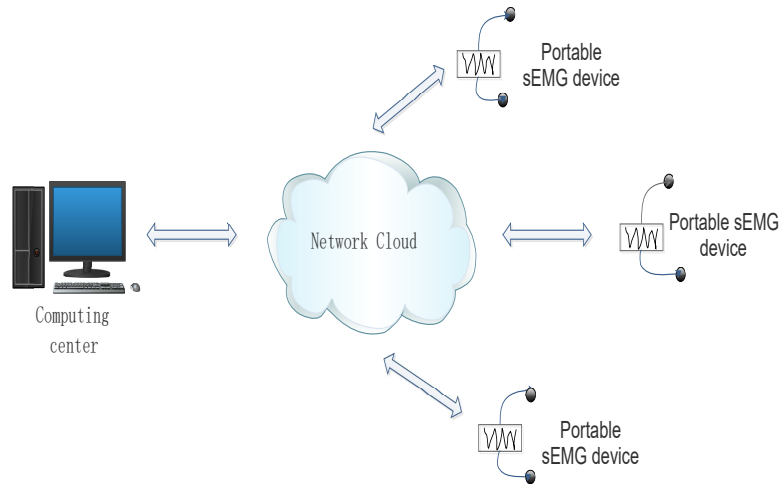


Figure 1: The CS identification based on sEMG and machine learning.

the acquisition of the sEMG signal become more portable and convenient. And, as the CS-related physiological signals sEMG ²²⁻²⁵ is non-intrusive and affordable, it is a promising direction that use the sEMG signal to provide the convenient, low-cost CS identification service as shown in the Figure 1.

The key of the harmless, convenient and low-cost CS identification is to classify subjects using sEMG signal. However, the higher-accurate, higher-sensitivity and higher-specificity CS identification is an challenging task because of the following three folds:

- The weak usability of the data: the instability of instruments³ and the long-term irregular

³In addition to the Ag/AgCl electrode, the conductive gel is also used to collect data so that the large noise and errors are easily introduced ⁴

movement habits of the subjects result in inaccurate measurement results, and the peeling of the electrode caused by the interference of the sweat lead the incompleteness of the single sample data. The inaccurate and incompleteness of the data directly affect the data quality, increase the difficulty of model's training, even affect the final classification performance and generalization performance.

- High dimension and large dimension difference: the dimension of the sEMG sample are hundreds of thousands, the max, min and mean dimension of which respectively are 1453200, 36000, 328638. The high dimension and the large dimension difference of the sEMG sample will increase computational and storage overhead and affect the generalization ability of the classification algorithm when they are directly handled by the machine learning models.
- The complex spatial relationship: as the sEMG signals of the multiple muscles are related to the recruitment of multiple muscles in the cervical spine system, there is complex spatial relation between the sEMG signals of the different muscles. The relationship above is difficult to extract without the guidance of the expert knowledge and experience.

Currently, the performance of the CS identification using the sEMG signal is obtained by traditional machine learning model, the classification ability of which are bounded by the limited computational units of the shallow learning algorithm⁴ as well as the limited feature design ca-

⁴The shallow learning algorithm refer to the traditional machine learning model, such as the support vector machine learning model (SVM), random forest (RF), the logistic regression (LR), boosting. The SVM, RF and boosting can be viewed structurally as the models with only one hidden layer node. The LR can be viewed structurally as the models without hidden layer node.

pability. Compared with traditional machine learning model, the deep learning are able to learn complex nonlinear function ^{26,27} by adding multiple hidden layers. In addition, it has been shown that different layers of the deep neural network could learn different representations of objects automatically ^{26,28}. What's more, the convolutional neural network, an deep learning neural network, can extract the local relationship of the data and have lots of prior knowledge to compensate for the data we don't have ²⁹⁻³¹, improving the performance of classification and enhancing the generalization ability of the model.

In this paper, we developed a method EasiCSDeep based on the convolutional neural network to provide convenient, low-cost and intelligent CS identification with state-of-the-art performance, using sEMG signal. The EasiCSDeep is a three-tier model: feature extraction, spatial relationship representation and classification algorithm. For the feature extraction, we employed five kinds of feature extraction methods to extract features of the sEMG and characterize the high dimension sEMG signal as comprehensively as possible with the low dimensional features, effectively reducing data dimensions while preserving the raw sEMG signal properties. For the spatial relationship representation, we reorganized the feature data into two-dimensional array data according to the anatomical location of the muscles that produces the sEMG signal as well as the type of activity involved, supporting the deep learning model to automatically extract relationship between the sEMG signals of the multiple muscles. For the classification algorithm, we proposed a multi-channels model EasiDeep with six processing channels to process the different kinds of data simultaneously. The EasiDeep retain the main features, reduce the number of parameters and automatically capture the dependency relationship without the domain knowledge, improving the

performance of the model. With the metric of accuracy, sensitivity, specificity and AUC, the EasiDeep achieves performance of 0.9708 in AUC, 97.22% in accuracy, 100.00% in sensitivity and 92.86% in specificity.

Our contributions are the following five aspects:

- To the best of our knowledge, this EasiCSDeep represents the first effort to employ the deep learning to analyze the sEMG data for intelligent CS identification.
- We employed five types of feature extraction methods to extract five types of the features, each type feature focus on the properties of an aspect of the sEMG data, and characterize the sEMG signal as comprehensive as possible, reducing data dimensions while preserving raw sEMG signal properties. And each type of feature extraction method focus on the properties of the signals in a different observation view.
- Inspired by the the First Law of Geography ³², we reorganized the data combined the knowledge of the anatomy and kinematics, to improve the performance of the EasiCSDeep.
- According to the feature types, the EasiDeep is developed to automatically extract the relationship without the expert knowledge and experience, and reduce the parameters of network while ensuring sufficient computing power of the network.
- Compared with previous state-of-the-art models in the same classification task, our algorithm achieves a significant improvement in performance on same data set to further reduce personal misdiagnosis rate, overall misdiagnosis rate and missed diagnosis rate.

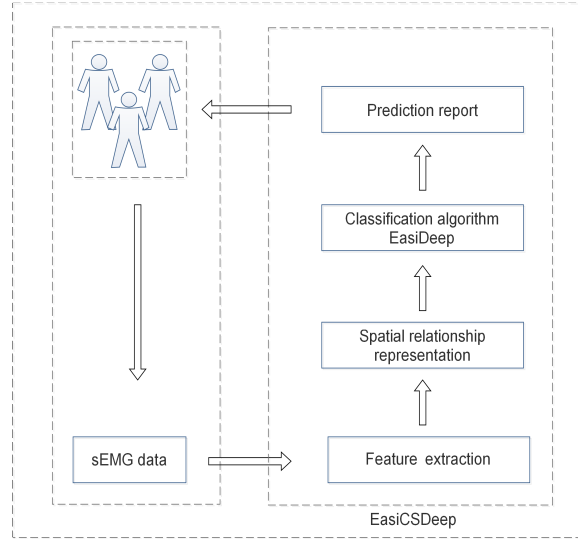


Figure 2: The CS identification method based on the EasiCSDeep and sEMG signal.

This work promotes the identification of physiological signal-based methods in a complex environment that is closer to the real application, and lays the foundation for the fine-grained classification of sEMG signals.

The paper is structured as follows. Section 2 summarizes the CS identification methods and machine learning algorithms. Section 3 describes the data set. Section 4 format the CS identification tasks. Section 5 introduces our proposed method EasiCSDeep. Section 6 evaluates and discusses the results. Section 7 concludes the paper and the future work.

2 Related Work

The CS, a chronic 'wear and tear' degenerative process of the cervical spine, affects the physical and mental health of human beings and poses a serious economic burden on society and individuals¹⁻³. Currently, its diagnosis mainly depend on intervention of medical resources including the professionals and medical instruments. There are many study on the methods of CS intelligent identification: image-based method, clinical symptoms-based method and physiological-signal-based method.

As the common means, the image-based intelligent CS identification attracted a lot of attention^{4,14,15}. The research³³ extracted 10 effective ROIs to establish X-ray symptom-disease table of CS, and developed the fuzzy calculation model based on the table above to classify CS, yielding approximately 80.33% accuracy. The research¹⁴ put forward a method based on maximum likelihood theory to classify the types of cervical spondylosis using X-ray, achieving the accuracy of 80% better than artificial X-ray reading method. Combined with the diffusion tensor imaging metrics, the research¹⁵ develop a support vector machine(SVM) classifier to classify the groups with the cervical spondylotic from the control groups, achieving the accuracy of 95.73%, sensitivity of 93.41% and specificity of 98.64%. The image-based CS intelligent recognition is an accurate and human resource-saving method. However, these minimal changes in the images in the early stage of the CS make visual diagnosis a difficult task and request more expert knowledge and experience. What's more, the intervention of medical instrument resources make the method relative costly and inconvenient.

For the physiological-signal-based method, it is well known that the sEMG physiological signal contains muscle lesion information, and are widely utilized to study muscle function and status of the patients with neck disease²²⁻²⁵. The research²² utilize the sEMG to explore cervical musculoskeletal function in female office workers with neck pain, the result of which is consistent with that there are the altered muscle recruitment strategy in the female office workers with neck pain. The research³⁴ employ the sEMG data to compare neck muscle activation patterns during and after a repetitive upper limb task between patients with idiopathic neck pain, whiplash-associated disorders and the control group, demonstrating that patients with neck pain have greater activation of accessory neck muscles that represent an altered pattern of motor control to compensate for reduced activation of painful muscles. The research³⁵ use the linear model to study the stability and repeatability of the sEMG index MF and MPF of the cervical muscle in CS patients as well as the healthy, and then employed the Student's t test to study the different of the index MF and MPF of the patients and the healthy, which demonstrates the correlation between cervical muscle and CS. However, there are few research on using the machine learning and sEMG signal to identify the CS. The research⁴ is the first work to identify CS using sEMG and AI. It proposed the convenient and effective data collection method and the machine learning identification model EasiAI including the feature extraction, feature selection and classification algorithm, which construct a dataset involving 179 subjects from multiple type CS and achieve the 91.43% in accuracy, 97.14% in sensitivity, 81.43% in specificity. It further demonstrates the feasibility of using sEMG and AI for cervical spondylosis screening to a certain extent. The performance of the EasiAI depend on feature engineering which requires expert knowledge and experience that lie in the deep

and comprehensive understanding of the development of the CS. However, the CS is an complex disease, every people is also an independent complex system, and the thorough and comprehensive exploration of the pathology of people's CS still need ongoing effort. It becomes more difficult to improve the performance of the model by constructing more features without the guidance of the expert knowledge and experience above.

The implementation of CS intelligent identification system above depends on the powerful statistical analysis approaches machine learning. The machine learning has been widely used in clinical data analysis to deal with the complicated data and has made great progress in medical^{36,37,37,38}. It is roughly divided into traditional machine learning and deep learning. When using traditional machine learning algorithms, we have to focus on designing appropriate features manually in addition to the conventional feature extraction methods^{26,28}. The design of the features require the professional knowledge and experience, which is even an challenging for domain experts. The deep learning are representation-learning methods with multiple levels of representation, which allows to be fed with raw data and automatically discover the representations needed for detection or classification^{27,37}. And it has brought about breakthroughs in processing images, video, speech and audio²⁷.

Although, the previous intelligent CS identification⁴ obtained 91.43% in accuracy, 97.14% in sensitivity, 81.43% in specificity. There are still room in improvement. It is essential and significant to reduce the overall misdiagnosis rate and missed diagnosis rate as much as possible for the population, and decrease the rate of misdiagnosis of individuals as much as possible.

In this paper, we seek to provide the convenient, low-cost and intelligent medical server of CS identification with state-of-the-art performance. It is a promising study that utilize the convenience of sensor technology and intelligent algorithms of artificial intelligence to transfer high-quality medical services from hospitals to families. It will promote the early detection and early treatment of the disease, reduce the cost and improve the cure rate. What's more, it will potentially alleviate the problem of difficulty and costliness to access medical service that is caused by the imbalance in the distribution of population and medical resources in China to some extent.

3 Dataset

The data set are acquired from 179 subject, 109 of which are the CS patients and 70 of which are the healthy. The sEMG signal from 6 muscles, which includes the left sternocleidomastoid(M_0), the left upper trapezius(M_1), the left cervical erector spinae(M_2), the right cervical erector spinae(M_3), the right upper trapezius(M_4) and the right sternocleidomastoid(M_5), were synchronously recorded when the subject completed the movements in the order of the bow(A_0), head backwards(A_1), left flexion(A_2), right flexion(A_3), left rotation(A_4), right rotation(A_5), and hands up(A_6), each movement of which is performed 3 times.

The movement A_j that is performed in $k - th$ time is represented as $A_{j,k}$ which generate a $S_{i,j,k}$. For a subject, the 3 $S_{i,j,k}(0 \leq i < 6)$ is obtained from the movement A_j and form a set that are denoted as AS_j . As shown in the Figure 3, the 7 $AS_j(0 \leq j < 7)$, each AS_j of which includes 3 $S_{i,j,k}(0 \leq i < 6)$, is obtained from the 7 movement A_j . And, respectively select 7

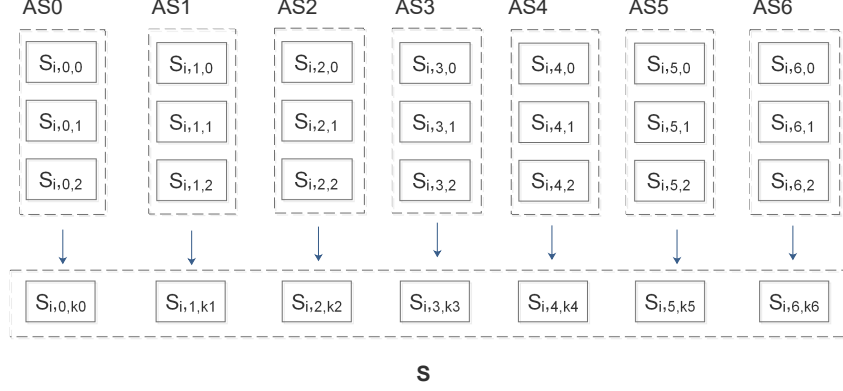


Figure 3: The formation of a sample S of a subject. The AS_i is the set of the $S_{i,j,k}$ from the movement A_j . The $S_{i,j,k}$ denote the signal generated on the muscle M_i ($0 \leq i < 6$) that is activated by the movement A_j in k -th time. $0 \leq K_0 < 3$, $0 \leq K_1 < 3$, $0 \leq K_2 < 3$, $0 \leq K_3 < 3$, $0 \leq K_4 < 3$, $0 \leq K_5 < 3$. And the $K_0, K_1, K_2, K_3, K_4, K_5$ are respectively set to random integer between 0 and 3.

$S_{i,j,k}$ ($0 \leq i < 6$) from 7 AS_j , and splice the 7 $S_{i,j,k}$ ($0 \leq i < 6$) in the order of $j = 0, j = 1, j = 2, j = 3, j = 4, j = 5, j = 6$ to form a sample S . The 2187 (1×3^7) samples are obtained from a subject, and the 391473 (179×3^7) samples are obtained from the 179 subjects. The sample is represented as S in the Formula 1- 2.

$$S = \begin{bmatrix} S_{0,0} & S_{0,1} & S_{0,2} & S_{0,3} & S_{0,4} & S_{0,5} & S_{0,6} \\ S_{1,0} & S_{1,1} & S_{1,2} & S_{1,3} & S_{1,4} & S_{1,5} & S_{1,6} \\ S_{2,0} & S_{2,1} & S_{2,2} & S_{2,3} & S_{2,4} & S_{2,5} & S_{2,6} \\ S_{3,0} & S_{3,1} & S_{3,2} & S_{3,3} & S_{3,4} & S_{3,5} & S_{3,6} \\ S_{4,0} & S_{4,1} & S_{4,2} & S_{4,3} & S_{4,4} & S_{4,5} & S_{4,6} \\ S_{5,0} & S_{5,1} & S_{5,2} & S_{5,3} & S_{5,4} & S_{5,5} & S_{5,6} \end{bmatrix}, (0 \leq i < 6, 0 \leq j < 7) \quad (1)$$

The i represent the muscle M_i , the j represent the movement A_j . The $S_{i,j}$ denote the signal generated on the muscle M_i in movement A_j .

$$S_{i,j} = \begin{bmatrix} p_1 & p_2 & \dots & p_n \end{bmatrix}, \quad (2)$$

Here, p_n is a value converted from the electrical signal.

4 The Formalization of the CS identification task

In order to identify CS patients from the healthy, our task is described as follows. The data set from the subjects are denoted as D . Let (X_i, y_i) , ($i \in \{1, \dots, N\}$) denotes the i th sample in the data set D , where the X_i is the sEMG data and the y_i is the label with

$$y_i = \begin{cases} 0 & X_i \text{ is sample of the healthy} \\ 1 & X_i \text{ is sample of the patient} \end{cases}$$

Our classification task is transformed to minimize the objective function $L(W)$ in the Formula 3.

$$L(W) = \sum_{i=1}^n \text{loss1}(X_i, y_i; W) + \sum_{i=1}^n \text{loss2}(X_i, y_i; W) + F(W) \quad (3)$$

The n denotes the number of the samples and the W is the parameters of the model. We employed the softmax function as the last output layer and the softmax cross-entropy function $\text{loss1}(X_i, y_i; W)$ as the loss function so that the health status and illness status can be independently optimized. Let $p_j(X_i, y_i; W) (j \in \{0, 1\})$ denotes the j th input of the softmax layer, then the j th activation of the softmax layer is $y_j(X_i, y_i; W)$ in the Formula 4.

$$y_j(X_i, y_i; W) = \frac{e^{p_j}}{\sum_{i=1}^j e^{p_i}} \quad (4)$$

The softmax cross-entropy function $loss1(X_i, y_i; W)$ is shown in Formula 5,

$$loss1(X_i, y_i; W) = -\hat{y}_i \times \sum_{i=1}^n \times \ln y_i \quad (5)$$

where the \hat{y}_i is the true value and y_i is the prediction value. The \hat{y}_i , the value of which is 0 or 1 at the same time, make sure that only one label is optimized independently. In order to make the predicted value y_i as close as possible to the true value \hat{y}_i , we simultaneously minimize the loss function $loss2(X_i, y_i; W)$ in Formula 6. In addition, we employed the classic L_2 regularized loss function $F(W)$ to counter overfitting in Formula 7,

$$loss2(X_i, y_i; W) = \sum_{i=1}^n (y_i - \hat{y}_i)^2 \quad (6)$$

$$F(W) = \alpha \times \|W\|_2^2 \quad (7)$$

where the α is the regularization parameter. We divide the train data set, validation data set and test data set by the ratio of 3:1:1 and make sure that the sample from a subject only appears in one data set.

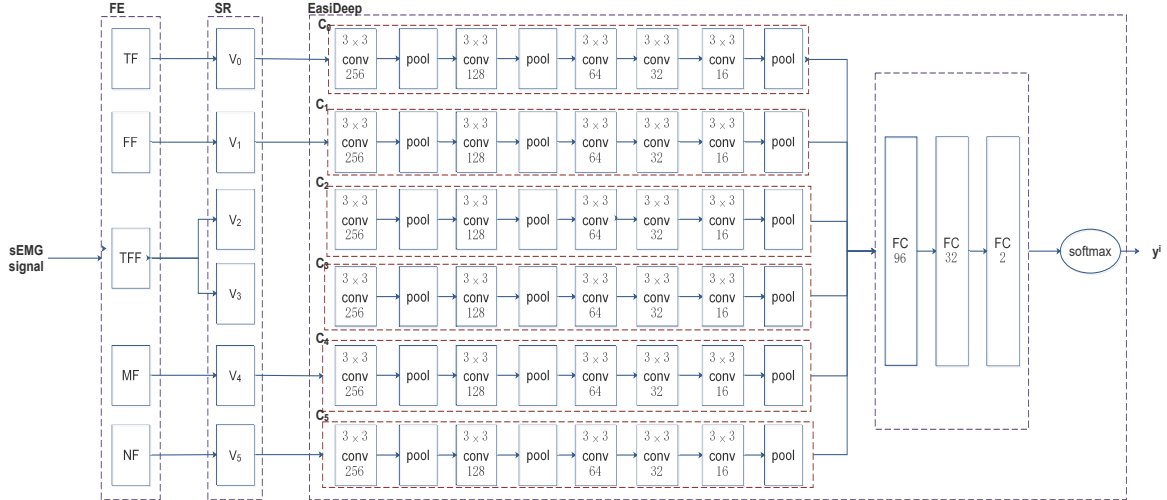


Figure 4: The EasiCSDeep.

5 The Methodology

In this section, we elaborate our proposed EasiCSDeep framework. As shown in Figure 4, the EasiCSDeep consists of the feature extraction FE , spatial relationship representation SR and classification algorithm EasiDeep.

The Feature extraction Faced with the high dimensionality and weak usability of the sEMG data, five types feature extraction methods, which includes time-domain methods (TM), frequent-domain methods (FM), the time-frequency method (TFM), the model-based methods (MM) and nonlinear entropy feature extraction method (NM), are used to extract the features and characterize the sEMG signal. Each type of the feature extraction method focus on the properties of the signals

in the different observation view.

Time-domain method The sEMG data is treated as the physical signal values on the time axis in time domain, the variation property of which is usually represented by the statistical feature such as the the average, variance, maximum and minimum etc. The time-domain methods are used to extract the feature above, which consider the sEMG signal as a random signal, the mean value of which is zero and the variance of which varies with the intensity of the signal. In this paper, we extracted 11 time-domain features from the sEMG signal $S_{i,j}$, forming features set $TF_{i,j}$. The $TF_{i,j}$ includes *mean*, *var*(variance), *std*(standard deviation), *mode*(the most common value), *max*(maximum value), *min*(minimum value), *over_zero*, *range*, *aemg*(averaged electromyogram), *iemg*(integrated electromyogram), *rms*(root mean square). The 11 types of features are extracted by the 11 calculation methods.

$$mean = 1/n \sum_{i=1}^n p_i \quad (8)$$

$$range = max - min \quad (9)$$

$$iemg = \sum_{i=1}^n |p_i - mean| \quad (10)$$

$$aemg = 1/n \sum_{i=1}^n |p_i - mean| \quad (11)$$

$$rms = 1/n \sum_{i=1}^n p_i^2 \quad (12)$$

Frequency domain method The frequency-domain analysis method focus on variation characteristics of the myoelectric signals in the frequency domain, the characteristics of which can be denoted as the frequency-domain features. In this paper, we utilized the fourier transform to convert the sEMG signal $S_{i,j}$ into $SF_{i,j}$, and extracted 14 frequency-domain feature values: dc (direct current), $mean$, var , std , $skew$ (skewness), $kurt$ (kurtosis), $entropy$, s_mean (shape mean), s_std (shape standard deviation), s_var (shape variance), s_skew (shape skewness), s_kurt (shape kurtosis), mf (median frequency), mpf (mean power frequency). The frequency domain feature set $FF_{i,j}$ are obtained.

$$SF_{i,j} = \left[x_0, x_1, \dots, x_{k-1} \right], \quad (13)$$

$$a = \text{int}(k/2) + 1 \quad (14)$$

$$dc = x_0 \quad (15)$$

$$skew = \frac{1}{a} \sum_{i=1}^a ((x_i - mean)/std)^3 \quad (16)$$

$$kurt = \frac{1}{a} \sum_{i=1}^a ((x_i - mean)/std)^4 - 3 \quad (17)$$

$$s_mean = \frac{\sum_{i=1}^a ix_i}{\sum_{i=1}^a x_i} \quad (18)$$

Time-frequency domain method Unlike the time domain and the frequency domain, the time-frequency domain method focus on both the time variation characteristic and frequency distribution simultaneously. Different from the features in time domain or frequency domain, the sEMG are able to be represented by the wavelet coefficients generated in the process of the wavelet transform³⁹. In this paper, we firstly use the famous method discrete wavelet transform(DWT) to

decompose sEMG signal at 5 levels. Then, we extracted the approximation coefficients C_h ⁵ at level 5. Meanwhile, we respectively extracted the detail coefficients $C_{l,5}, C_{l,4}, C_{l,3}, C_{l,2}$ ⁶ at the level 5, 4, 3, 2. Finally, we extracted the feature c_{max} , singular value, and c_{energy} from the $C_h, C_{l,5}, C_{l,4}, C_{l,3}, C_{l,2}$ respectively. Each sEMG signal $S_{i,j}$ can be represent by 15 features above. The TFF_WT_i, j are obtained from $S_{i,j}$.

$$c_{max} = Max [\log_{10}(x), x \in C] \quad (19)$$

$$C_{energy} = \log_{10} \frac{\sqrt{\sum_{x \in C} x^2}}{|C|} \quad (20)$$

In addition, the signal is also decomposed into the coefficients by the wavelet packet decomposition(WPD) when feed into the low (L) and high (H) filter at the same time⁴⁰ in the Equation 21.

$$\psi_{j,k}^i(t) = 2^{-j/2} \psi^i(2^{-j}t - k), \quad (i = 1, 2, \dots, j^n) \quad (21)$$

$$\psi^{2i}(t) = \frac{1}{\sqrt{2}} \sum_{k=-\infty}^{\infty} h(k) \psi^i\left(\frac{t}{2} - k\right) \quad (22)$$

$$\psi^{2i+1}(t) = \frac{1}{\sqrt{2}} \sum_{k=-\infty}^{\infty} g(k) \psi^i\left(\frac{t}{2} - k\right) \quad (23)$$

⁵only the coefficients which is large than 0 will be extracted

⁶only the coefficients which is large than 0 will be extracted

Here, i is the modulation parameter, j is the dilation parameter, k is the translation parameter, n is the level of the decomposition, $h(k)$ and $g(k)$ are the quadrature mirror filters⁴¹.

$$c_{j,k}^i = \int_{-\infty}^{\infty} f(t)\psi_{j,k}^i(t)dt \quad (24)$$

As shown in the Formula 24, the $c_{j,k}^i$ is the coefficients of the WPD, and $f(t)$ is the signal to be decomposed⁴¹. In this paper, we set the level of the decomposition to $n = 3$ and each sEMG signal is represented by 8 coefficients. After the WPD coefficients extraction, we obtained the feature set TFP_WP_i, j from $S_{i,j}$.

The model-based method For the model-based methods, we focus on the character of the data joint distribution. Usually, the $x + 1$ -th value of the sEMG have a relationship with the previous signals, and the relationship above is represented by the coefficient of the model. The Autoregressive (AR) model, a popular feature extraction method, is widely applied for the physiological signals analysis to characterize the joint distribution of the sEMG by representing the sEMG signal as the coefficients of the model⁴² as shown in the Equation 25.

$$y(t) = \sum_{i=1}^p \phi_i y(t-i) + \varepsilon_i \quad (25)$$

Here, $y(t)$ is the signal to be modeled, and ϕ_i are the model coefficients, ε_i is white noise.

The p , which determines the number of the coefficients and the complex of the model, is the order of the AR model. We set the $p = 10$ and $p = 4$, and train two AR model by the sEMG signal respectively. Thus, each sEMG signal $S_{i,j}$ is represented as $MF_{i,j}$ including 14 RA model coefficients above.

Nonlinear feature extraction method As the sEMG signals are generated by the exchange of ions across the muscle membranes, the states of the exchange of ions are detected by the electrodes ⁴³, and the change of the states reflect the degree of mess of the muscle's activity. We use entropy to describe the degree of the mess of the muscle's activity. In detail, each value of the sEMG signal represent a state, and the entropy is denoted as Equation 26.

$$entropy = \sum_{i=1}^n p_i \log(p_i) \quad (26)$$

Here, the n is the number of the states in the system, and p_i is the probability of the state i in the system. The set $NF_{i,j}$ are generated after we extracted the *entropy* index from the sEMG signal $S_{i,j}$.

Spatial relationship representation In this paper, we obtained the six kinds of features set: TF ⁷, FF ⁸, TF_{WT} ⁹, TF_{WP} ¹⁰, MF ¹¹, NF ¹² from a sample including 6×7 sEMG signals $S_{i,j}$. For the convenience of introduction, we respectively represented TF , FF , TF_{WT} , TF_{WP} , RF , and SF as F_0 , F_1 , F_2 , F_3 , F_4 , F_5 .

Inspired by that the First Law of Geography³², using the regions with strong correlation to predict the CS can improve the performance of the machine learning algorithms⁴⁴. What's more, considering the relationship between the muscles activated by the same movement, we reshape the view features data F_k into the V_k , and the V_k meets the following requirements: (1)the data on the muscles involved in the same movement are put together. (2)the data on the muscles whose physiological position are closer are put together closer.

As shown in Formula 27, we reshape the features F_k into V_k . The i th row of the V_k are forming by stitching the $F_{i,j}$ in the order of the j from 0 to 6. The j th column are forming by splicing the $F_{0,j}$, $F_{5,j}$, $F_{2,j}$, $F_{3,j}$, $F_{1,j}$ and $F_{4,j}$ in turn.

⁷ The TF includes $6 \times 7 \times 11 TF_{i,j}$.

⁸The FVF includes $6 \times 7 \times 14 FF_{i,j}$.

⁹The TF_{WT} includes $6 \times 7 \times 15 TFF_{WT_i,j}$.

¹⁰The TF_{WP} includes $6 \times 7 \times 8 TFF_{WP_i,j}$.

¹¹The MF includes $6 \times 7 \times 14 MF_{i,j}$.

¹²The NF includes $6 \times 7 \times 1 NF_{i,j}$.

$$V_k = \begin{bmatrix} F_{0,0}, & F_{0,1}, & F_{0,2}, & F_{0,3}, & F_{0,4}, & F_{0,5}, & F_{0,6} \\ F_{5,0}, & F_{5,1}, & F_{5,2}, & F_{5,3}, & F_{5,4}, & F_{5,5}, & F_{5,6} \\ F_{2,0}, & F_{2,1}, & F_{2,2}, & F_{2,3}, & F_{2,4}, & F_{2,5}, & F_{2,6} \\ F_{3,0}, & F_{3,1}, & F_{3,2}, & F_{3,3}, & F_{3,4}, & F_{3,5}, & F_{3,6} \\ F_{1,0}, & F_{1,1}, & F_{1,2}, & F_{1,3}, & F_{1,4}, & F_{1,5}, & F_{1,6} \\ F_{4,0}, & F_{4,1}, & F_{4,2}, & F_{4,3}, & F_{4,4}, & F_{4,5}, & F_{4,6} \end{bmatrix}, \quad (27)$$

The EasiDeep For each kind of data V_i , we employed channels C_i to process it. The channel consists of the 5 convolution layers and 3 pooling layers. The transformation at each convolution layer k is defined as follows:

$$Y^k = f(Y^{k-1} * W^k + b^k) \quad (28)$$

The Y^k is the output of the k -th layer, the $*$ denotes the convolutional operation, the f is the activation function. In this paper, we use the Relu function as the activation function. The W^k and b^k respectively represent parameters and biases of the convolution layer k . The transformation at each pooling layers k is defined as follows:

$$Y^i = g(Y^{i-1}) \quad (29)$$

The g is the pooling function. In this paper, we use the max function as the pooling function. After the channels, the outputs Y^k are flatten and stitched into a feature vector FY^k ($FY^k \in$

$R^{S_i \times S_j \times 1}$), then feed into the two fully connected layers to reduce the dimension, each fully connected layer i of which is defined as:

$$FY^{(i)} = f(FY^{i-1} \times W^i + b^i) \quad (30)$$

The W^i and b^i respectively are the parameter and biases of the fully connected layer i . Finally, the output of the last fully connected layer is feed into the softmax layer.

$$Y^{(i)} = softmax(FY^{i-1} \times W^i + b^i) \quad (31)$$

The $Y^{(i)}$ is a vector (y_0^i, y_1^i) . The y_0^i and y_1^i are greater than 0 and is less than 1, and the sum of y_0^i and y_1^i is equal to 1. The y_0^i denotes the probability that the sample is the healthy. The y_1^i denotes the probability that the sample is the CS suffer.

Algorithm and Optimization As the Algorithm 1 shown, we firstly extract the features from the raw sEMG in different views respectively. Then, the EasiCSDeep is trained by the back-propagation and the AdamOptimizer.

6 Experiments Results, Evaluation and Discussion

With the metric of accuracy, sensitivity, specificity and AUC(the area under the sensitivity and specificity curve)^{38,45}, we validated the effectiveness of the EasiCSDeep in three ways: (a)compare the EasiCSDeep with other machine learning models.(b) compare the EasiCSDeep with the various

Algorithm 1 EasiDeep Training Algorithm

Input: The sEMG of samples: $\{X_0, X_1, \dots, X_{n-1}\}$;

The label of the samples: $\{y_0, y_1, \dots, y_{n-1}\}$.

Output: Learned EasiCSDeep model

```
1: //construct training instances
2:  $D \leftarrow \phi$ 
3: for all sEMG of samples do
4:   the  $TF$  features in the  $TM$  method
5:   extracting the features  $V_1$  in the  $FV$  view.
6:   extract the  $FF$  features in the  $FM$  method
7:   extract the  $TF F_{WT}$  features in the  $TFM$  method
8:   extract the  $TF F_{WP}$  features in the  $TFM$  method
9:   extract the  $NF$  features in the  $NM$  method
10:  represent  $\{TF, FF, TF F_{WT}, TF F_{WP}, MF, NF\}$  into  $\{V_0, V_1, V_2, V_3, V_4, V_5\}$ 
11:  //y is the label of the sample
12:  put an training instance  $(\{V_0, V_1, V_2, V_3, V_4, V_5\}, y)$  into  $D$ 
13: end for
14: // train the model
15: initialize all learnable parameters  $\theta$  EasiDeep
16: repeat
17:   select a batch of instances  $D_b$  from  $D$ 
18:   find  $\theta$  by minimizing the Formula 3 with  $D_b$ 
19: until stopping criteria is met
```

configurations of the channel combination.(c)compare the EasiCSDeep with the various configurations of filter size.

The metrics The good intelligent CS identification model primarily are able to decrease the rate of misdiagnosis of individuals as much as possible, and reduce the overall misdiagnosis rate and missed diagnosis rate as much as possible for the population. The higher accuracy is, the lower the rate of misdiagnosis of individuals. The higher sensitivity and specificity, the lower the overall missed diagnosis rate and misdiagnosis of the population are. So we use the accuracy, sensitivity and specificity as the metrics in our paper, and they are defined as follows.

$$accuracy = \frac{tp + tn}{p + n} \quad (32)$$

$$sensitivity = \frac{tp}{p} \quad (33)$$

$$specificity = \frac{tn}{n} \quad (34)$$

where the 'tp' is the number of correctly predicted patient with CS, p is the number of patient with CS shown, 'tn' is the number of correctly predicted healthy people free of CS, and the 'n' is the number of healthy free of CS shown. The higher the sensitivity is, the lower the missed diagnosis rate is. The higher the specificity is, the lower the misdiagnosis rate is. Furthermore, the high sensitivity boosts the early detection of the more patient population. The higher specificity decreases the misdiagnosis rate.

Models for Comparison We compared the EasiCSDeep with the traditional machine learning models: logistic regression(LR), support vector machine(SVM), random forest(RF) and EasiAI on the same data set in the same classification task. In addition, we also considered the comparison

with a typical deep learning model DL_{cnn} based on CNN which was developed in our paper. The details on the models above is as follows:

- LR: The logistic regression is a classic linear regression method. The output of the LR is between 0 and 1. The closer the output value is to 1, the more likely the sample is positive.
- SVM: The SVM is a classic two-class model. It can find the optimal hyperplane of the n -dimensional space to separate the positive and negative samples.
- RF: The RF is a classic bagging-based ensemble learning algorithm, which consists of multiple decision trees. The prediction result is voted by all the decision trees.
- EasiAI⁴: The EasiAI is an ensemble learning algorithm based on the GBDT (gradient boosted regression tree), which includes the feature extraction, feature selection and classification algorithm.
- DL_{cnn} : The architecture of DL_{cnn} is the same as C_i . The DL_{cnn} consists of the 5 convolutional layers, 3 pooling layers, 3 fully connected layers and 1 softmax function.

Preprocessing and Parameters We used the mean of the features to fill in the missing data, and employed the StandardScaler provided by the sklearn.preprocessing (0.19.1) to process the data set. In addition, the label is transformed into the two-dimensional array, using the one-hot encoding.

All the experiments in the paper were run on the cluster with four NVIDIA Corporation GP102 [TITAN Xp] (rev a1). The python (3.6.5) and tensorflow (1.1.0) were used to implement

the deep learning algorithms in the paper. The number of the convolution layer is 5. The pooling layer number is 3, and the fully connected layer number is 3. The activation function for each layer is Relu, and the batch normalization is used to process the input of the Relu. The filter size of each convolution layer is 5×5 . The kernel size of pooling layer is 2×2 . The kernel number of the convolution layers respectively are 256, 128, 64, 32, 16. The number of neural units in the fully connected layer respectively is 96, 32, 2. The batch size is set to 148, and the learning rate is 0.00006. The max epoch is 10000. The 60% of the samples is used for training the model, 20% is used as the validation data set for selecting the model with the best performance. The early-stop was also applied when training the model, the round of which is less than 1500 in all the experiments.

Performance Comparison

6.0.1 Comparison with the other machine learning models

As detailed in Table 1, the EasiCSDeep achieved the highest AUC 0.9708, the highest accuracy 97.22%, the highest sensitivity 100% and the highest specificity 92.86%. We compared the EasiCSDeep with the traditional machine learning model of LR, SVM, RF and EasiAI. Compared with the LR with the lowest sensitivity, the EasiCSDeep obtained 10.65, 11.08, 10.00 and 0.0508 percentage point improvement in accuracy, sensitivity, specificity and AUC. Compared with the SVM with the lowest accuracy, the EasiCSDeep got 11.22, 10.22, 12.86 and 0.0508 percentage point improvement in accuracy, sensitivity, specificity and AUC. Compared with the RF with the

lowest specificity, the accuracy, sensitivity, specificity and AUC has been improved by 9.57, 6.58, 14.29 and 0.0308 percentage point. Compared with the previous state-of-the-art identification model EasiAI, the EasiCSDeep obtained 6.2, 2.86, 11.43 and 0.0208 percentage point improvement in classification accuracy, sensitivity, specificity and AUC.

In addition, we compared the EasiCSDeep with the deep learning model DL_{cnn} . The EasiCSDeep obtained 5.79%, 4.75%, 8.7%, 0.0014 improvement in the accuracy, sensitivity, specificity and AUC. Overall, the EasiCSDeep provides the state-of-the-art classification performance, proving that the deep learning algorithm outperform the traditional machine learning. Multi-channel models (EasiCSDeep) have better classification performance than single-channel model(DL_{cnn}).

6.0.2 Comparison of the EasiCSDeep with the various channel combination

We evaluate the EasiCSDeep with all the configurations of the channel combination. The channel C_0, C_1, C_2 , which are fed with the feature data extracted in the commonly methods, are considered as the basis channels. Combine the basic channels and other channels C_3, C_4 and C_5 , and compare the performance of the model with different channel combination. The 8 models with various channel combination are shown in the Table 2. In the three-channels model with the combination of channel C_0, C_1, C_2 , the accuracy is 78.25%. In the three-channels model with the combination of channel C_0, C_1, C_2, C_3 , the accuracy is 83.33%. In the five-channels model with the combination of channel C_0, C_1, C_2, C_4, C_5 the accuracy is 86.11%. In the six-channels model with the combination of channel $C_0, C_1, C_2, C_3, C_4, C_5$ the accuracy is 97.22%. It is concluded that the addition of the

channel C_3 improve the accuracy to a certain extent. In all the four-channels models, the highest accuracy is 86.11%, the lowest accuracy is 80.00% and the mean accuracy is 83.15% which is large than 78.25% of three-channel model. In all the five-channels models, the highest accuracy is 94.44%, the lowest accuracy is 86.11% and the mean accuracy is 89.81% which is large than the mean accuracy 83.15% of the four-channels models. The EasiCSDeep with six channels provides the highest accuracy 97.22%. Overall, the highest and lowest accuracy rate rise as the number of the channels increases. The results validate the effectiveness of the six-channels EasiCSDeep. As the different channel is almost used to process a type of the feature data, which focus on the property of one aspect of sEMG signal, it is also indicated that the sEMG signal of CS is an complex data which have the variation characters.

6.0.3 Comparison of the EasiCSDeep with the various filter size

We assess our model EasiCSDeep with the various configurations of filter size in the Table 3. As detailed in Table 3, the EasiCSDeep obtain the highest accuracy 97.22% when the filter size is (5, 5). When the filter size is (2, 2), the accuracy is lowest 83.67%. In general, the accuracy rises as the filter size increases. It concluded that the spatial relationship representation has an positive effect on the CS classification task, and it demonstrated that using the regions with strong correlation to predict the CS can improve the performance of the machine learning algorithms⁴⁴.

In turn, two conclusions are summarized: (1)there are strong relationship between the sEMG signal of the six muscles activated by the same movement.(2)there are strong relationship between

Table 1: The performance comparison between the EasiCSDeep and previous research.

Model	AUC	Accuracy	Sensitivity	Specificity
LR	0.9200	86.57%	88.92%	82.86%
SVM	0.9200	86.00%	89.78%	80.00%
RF	0.9400	87.65%	93.42%	78.57%
EasiAI	0.9500	91.02%	97.14%	81.43%
DL_{cnn}	0.9694	91.43%	95.25%	84.16%
EasiCSDeep	0.9708	97.22%	100.00%	92.86%

Table 2: The comparison between different EasiCSDeep models with different channel combination.

Index	C_0	C_1	C_2	C_3	C_4	C_5	Accuracy
0	✓	✓	✓				78.25%
1	✓	✓	✓	✓			83.33%
2	✓	✓	✓		✓		86.11%
3	✓	✓	✓			✓	80.00%
4	✓	✓	✓	✓	✓		94.44%
5	✓	✓	✓	✓		✓	88.89%
6	✓	✓	✓		✓	✓	86.11%
7	✓	✓	✓	✓	✓	✓	97.22%

the sEMG signal of the muscles whose physiological position are closer. It can be further explained by that:(1) the sEMG of the six muscles are affected by the muscles recruitment pattern. (2) there are differences in muscle recruitment patterns between the CS and the healthy.

7 Conclusions and future work

In this paper, we have proposed and developed an novel multi-channel model EasiCSDeep based on deep learning using sEMG signal that can be easily acquired by the portable device. The EasiCSDeep comprehensively characterizes the high dimension sEMG signal with the low dimension features data, reorganize data into matrix format to support the computation of the deep learning, and developed the EasiDeep with six-channels to process the five types of feature data simultaneously which are able to automatically capture the dependency relationship and boost the performance of the model. Compared with the previous study, the EasiCSDeep provides the state-of-the-art performance, outperforming the traditional learning algorithms. The accuracy, sensitivity and specificity have been respectively improved by 6.2, 1.78 and 11.43 percentage points. For individuals, the improvement in the accuracy decrease the misdiagnosis rate. For the population, the improvement in sensitivity boosts the early detection of the more patient population. The improvement in specificity decreases the misdiagnosis rate of the healthy free of the CS. It is a very significant improvement which promotes the development of intelligent CS screening services in complex environments and boosts the study of the fine-grained classification models for the precision CS screening services.

In the future, we will build a more comprehensive database of CS which involves a variety of the CS subtype and includes multiple data types including images and medical records as well as expert knowledge and experience. Based on the database above, we will develop more intelligent and fine-grained classification system for CS screening to provide the convenient, low-cost and high-quality medical server, improving disease cure rate and reducing cost. Meanwhile, we look forward to discovering more objective physiological indicators of cervical spondylosis development to further provide assistance for its diagnosis and treatment.

1. Matz, P. *et al.* Joint section on disorders of the spine and peripheral nerves of the american association of neurological surgeons and congress of neurological surgeons. *J Neurosurg Spine* **11**, 157–169 (2009).
2. Kotil, K. & Bilge, T. Prospective study of anterior cervical microforaminotomy for cervical radiculopathy. *Journal of Clinical Neuroscience* **15**, 749–756 (2008).
3. Cai, Z. *et al.* Trend of the incidence of cervical spondylosis: decrease with aging in the elderly and increase with aging in the young and the adults. *Int J Clin Exp Med* **9**, 14329–14336 (2016).
4. Wang, N. A convenient non-harm cervical spondylosis intelligent identity method based on machine learning. *bioRxiv* 264663 (2018).
5. Fengyan, L., Jing, Y., Yanming, X. & Deyou, C. Comorbidities and medication of patients with cervical spondylosis: A study based on hospital information system. *Chinese General Practice* **20**, 980–983 (2017).

6. Shaoqun, Z. & Yikai, L. History of cervical spondylosis research. *Chinese Journal of Rehabilitation Medicine* **31**, 1273–1276 (2016).
7. Liu, Z. *A study on the relationship of cervical spondylotic radiculopathy between lesions of signs and symptoms*. Master's thesis, (2013).
8. Health, N. & of PRC, F. P. C. *China Health and Family Planning Statistics Yearbook* (Peking Union Medical College Press, 2017).
9. world bank, T. Health data. <http://datatopics.worldbank.org/health/health> (2017).
10. of Statistics, N. B. Census data. <http://www.stats.gov.cn/tjsj/pcsj> (2010).
11. Hou, X., Deng, X. & Zhao, W. research on status and countermeasures of medical and health information resources allocation in china. *China Health Resources* 274–277 (2014).
12. AN, Y. Characters and improvement strategies of distribution of high-quality medical resource. *China Health Quality Management* **18**, 110–113 (2011).
13. Ying, Z., Zheng, H., Yang, Q., Wang, Z. & Wei, J. Thinking of good quality medical resources issues of large urban hospitals sinking to the country. 1–3 (2013).
14. Yu, X., Liu, M., Meng, L. & Xiang, L. Classifying cervical spondylosis based on x-ray quantitative diagnosis. *Neurocomputing* **165**, 222–227 (2015).

15. Wang, S., Hu, Y., Shen, Y. & Li, H. Classification of diffusion tensor metrics for the diagnosis of a myelopathic cord using machine learning. *International journal of neural systems* **28**, 1750036 (2018).
16. ZHOU, W. *et al.* Development, fabrication, and applications of biomedical electrodes. *Chinese Science Bulletin* **60**, 1352–1360 (2015).
17. Lee, B. W., Lee, C., Kim, J. & Lee, M. Comparison of conductive fabric electrode with electromyography to evaluate knee joint movement. *IEEE Sensors Journal* **12**, 410–411 (2012).
18. Zhang, Z., Tao, D., Gen, Y. *et al.* Performance analysis of textile sensors in control of multi-functional myoelectric prostheses. *Bulletin of Advanced Technology Research* **4**, 1–6 (2010).
19. Merletti, R., Botter, A., Troiano, A., Merlo, E. & Minetto, M. A. Technology and instrumentation for detection and conditioning of the surface electromyographic signal: state of the art. *Clinical Biomechanics* **24**, 122–134 (2009).
20. Kim, S. *et al.* Influence of contact pressure and moisture on the signal quality of a newly developed textile ecg sensor shirt. In *Medical Devices and Biosensors, 2008. ISSS-MDBS 2008. 5th International Summer School and Symposium on*, 256–259 (IEEE, 2008).
21. Grajales, L. & Nicolaescu, I. V. Wearable multisensor heart rate monitor. In *Wearable and Implantable Body Sensor Networks, 2006. BSN 2006. International Workshop on*, 4–pp (IEEE, 2006).
22. Johnston, V., Jull, G., Souvlis, T. & Jimmieson, N. L. Neck movement and muscle activity characteristics in female office workers with neck pain. *Spine* **33**, 555–563 (2008).

23. Madeleine, P., Xie, Y., Szeto, G. P. & Samani, A. Effects of chronic neck–shoulder pain on normalized mutual information analysis of surface electromyography during functional tasks. *Clinical Neurophysiology* **127**, 3110–3117 (2016).
24. Johnston, V., Jull, G., Darnell, R., Jimmieson, N. & Souvlis, T. Alterations in cervical muscle activity in functional and stressful tasks in female office workers with neck pain. *European journal of applied physiology* **103**, 253–264 (2008).
25. Falla, D., Farina, D., Dahl, M. K. & Graven-Nielsen, T. Muscle pain induces task-dependent changes in cervical agonist/antagonist activity. *Journal of Applied Physiology* **102**, 601–609 (2007).
26. Zhou, X.-X. *et al.* pdeep: Predicting ms/ms spectra of peptides with deep learning. *Analytical chemistry* **89**, 12690–12697 (2017).
27. LeCun, Y., Bengio, Y. & Hinton, G. Deep learning. *nature* **521**, 436 (2015).
28. Zeiler, M. D. & Fergus, R. Visualizing and understanding convolutional networks. In *European conference on computer vision*, 818–833 (Springer, 2014).
29. Krizhevsky, A., Sutskever, I. & Hinton, G. Imagenet classification with deep convolutional neural. In *Neural Information Processing Systems*, 1–9 (2014).
30. Jarrett, K., Kavukcuoglu, K., LeCun, Y. *et al.* What is the best multi-stage architecture for object recognition? In *Computer Vision, 2009 IEEE 12th International Conference on*, 2146–2153 (IEEE, 2009).

31. Krizhevsky, A. & Hinton, G. Convolutional deep belief networks on cifar-10. *Unpublished manuscript* **40** (2010).
32. Tobler, W. R. A computer movie simulating urban growth in the detroit region. *Economic geography* **46**, 234–240 (1970).
33. Yu, X. & Xiang, L. Classifying cervical spondylosis based on fuzzy calculation. In *Abstract and Applied Analysis*, vol. 2014 (Hindawi, 2014).
34. Falla, D., Bilenkij, G. & Jull, G. Patients with chronic neck pain demonstrate altered patterns of muscle activation during performance of a functional upper limb task. *Spine* **29**, 1436–1440 (2004).
35. Zhao, Z. *Research on Symptoms Signs and Soft Tissue Changes of Neck Type of Cervical Spondylosis*. Ph.D. thesis, China Academy of Chinese Medical Sciences (2011).
36. Lezcana-Valverde, J. M. *et al.* Development and validation of a multivariate predictive model for rheumatoid arthritis mortality using a machine learning approach. *Scientific reports* **7**, 10189 (2017).
37. Miotto, R., Wang, F., Wang, S., Jiang, X. & Dudley, J. T. Deep learning for healthcare: review, opportunities and challenges. *Briefings in bioinformatics* (2017).
38. Esteva, A. *et al.* Dermatologist-level classification of skin cancer with deep neural networks. *Nature* **542**, 115 (2017).

39. Acharya, U. R. *et al.* Automated detection of premature delivery using empirical mode and wavelet packet decomposition techniques with uterine electromyogram signals. *Computers in biology and medicine* **85**, 33–42 (2017).
40. Alakus, T. B. & Turkoglu, I. Detection of pre-epileptic seizure by using wavelet packet decomposition and artificial neural networks. In *Electrical and Electronics Engineering (ELECO), 2017 10th International Conference on*, 511–515 (IEEE, 2017).
41. Shinde, A. & Hou, Z. A wavelet packet based sifting process and its application for structural health monitoring. *Structural Health Monitoring* **4**, 153–170 (2005).
42. Koçer, S. & Tümer, A. E. Classifying neuromuscular diseases using artificial neural networks with applied autoregressive and cepstral analysis. *Neural Computing and Applications* **28**, 945–952 (2017).
43. Altın, C. & Er, O. Comparison of different time and frequency domain feature extraction methods on elbow gestures emg. *European Journal of Interdisciplinary Studies* **5**, 35–44 (2016).
44. Yao, H. *et al.* Deep multi-view spatial-temporal network for taxi demand prediction. *arXiv preprint arXiv:1802.08714* (2018).
45. Baldi, P., Sadowski, P. & Whiteson, D. Searching for exotic particles in high-energy physics with deep learning. *Nature communications* **5**, 4308 (2014).

Table 3: The comparison between different EasiCSDeep models with different configuration of filter size.

Channels	Filter size	Pool size	Accuracy
6	(6,6)	(2,2)	86.11%
6	(5,5)	(2,2)	97.22%
6	(4,4)	(2,2)	88.89%
6	(3,3)	(2,2)	82.13%
6	(2,2)	(2,2)	80.56%